

## Shifts of Light Beams Due to Total Internal Reflection

Neil Ashby and Stanley C. Miller, Jr.

*Department of Physics and Astrophysics, University of Colorado, Boulder, Colorado 80302*

(Received 13 July 1972; revised manuscript received 3 November 1972)

A method for treatment of the transverse or longitudinal shifts of multiply internally reflected light beams is developed in terms of eigenfunctions for the reflection processes. Localized wave packets composed of plane-wave eigenfunctions are used to discuss the detailed structure of the shifted intensity distributions for several experimental conditions. With this approach image widths and over-all shifts, as well as splittings between images, can be calculated. The predictions are compared with the experimental results of Imbert and are found to agree with the observed transverse splitting between left and right circularly polarized light beams. Since the theory presented here disagrees with that proposed by Imbert in several respects, experiments are suggested which would distinguish between alternative theories.

### I. INTRODUCTION

Internally reflected light beams may undergo shifts of position in the plane of incidence (longitudinal) or normal to the plane of incidence (transverse) when reflection occurs near the critical angle for total internal reflection. The longitudinal shift was first studied by Goos and Hänchen<sup>1</sup>; in this case an unpolarized light beam which is multiply internally reflected between parallel reflecting surfaces is split into two plane-polarized beams with the beam which is polarized parallel to the plane of incidence being displaced more. The transverse shifts were first predicted by Fedorov,<sup>2</sup> and have recently been observed experimentally by Imbert.<sup>3,4</sup> Here different transverse shifts for left and right circularly polarized light are observed.

A number of different theoretical approaches have been used to study the longitudinal shifts. Artmann<sup>5</sup> was the first to use a stationary-phase argument to calculate the position of the shifted beam. Another theoretical approach has been based on consideration of energy flux within the evanescent wave.<sup>6</sup> A thorough discussion has been given by Lotsch,<sup>7</sup> based on an approximate solution of Maxwell's equations in which the amplitude depends on the coordinates transverse to the beam direction.

The transverse shift has been treated by the stationary phase method by Schilling<sup>8</sup>; however, he did not properly take into account the effect of phase shifts arising from the reflection process. The theoretical calculations of Costa de Beauregard,<sup>9</sup> Ricard,<sup>10</sup> and Imbert<sup>3,11</sup> are based on considerations of energy flux within the evanescent wave. Actually such calculations can predict at best only the centroid of the shifted beam; on this basis, for example, it is not possible to calculate details of

the intensity distribution within the multiply reflected beam.

This fact is easy to overlook, and has led de Broglie and Vigier<sup>12</sup> to suggest that photons possess rest mass. This has been refuted by Troup *et al.*<sup>13</sup> Also, Costa de Beauregard and Imbert<sup>14</sup> have pointed out that in the case of the longitudinal effect, the light beams of different plane polarizations do not interfere, so that an unpolarized light beam is split into two beams. Similarly, they argue that for the transverse effect, since right and left circularly polarized light beams will not interfere, unpolarized light will be split into two beams. The experiments of Imbert<sup>3,4</sup> appear to agree with predictions made by using energy-flux calculations.

One should instead be able to calculate these shifts by a straightforward application of Maxwell's equations, comparing the reflected wave with the incident wave. In this paper we shall carry out these calculations for a multiply reflected wave packet consisting of a superposition of plane waves. In general our results disagree with those of Imbert<sup>3</sup> and Ricard<sup>10</sup>; in particular, for the experimental conditions used by Imbert,<sup>3</sup> we find that both left and right circularly polarized light beams are shifted in the *same* direction, with a separation which is in agreement with the observations. For other experimental conditions the images are found to have a complicated structure, i.e., in some cases more than two images should be visible.

In Sec. II of this paper we develop the formalism required to describe multiple reflections in terms of eigenfunctions of the reflection process. In Sec. III we discuss a number of applications, such as reflection from metallic surfaces and reflection in the interior of a prism. Numerical calculations are carried out to find the detailed image structure.

## II. EIGENFUNCTIONS FOR MULTIPLE-REFLECTION PROCESSES

In this section we develop the necessary algebra for the description of multiple internal reflections. The phenomenon is well understood for a single reflection.<sup>15</sup> However, for the observation of longitudinal and transverse shifts many reflections must be used. Therefore, as in the discussion of reflection of electrons,<sup>16</sup> it will be convenient to express the results in a form in which eigenfunctions for the reflection processes appear.

Consider, as in Fig. 1, a wave packet of light of frequency  $\omega/2\pi$  incident from the interior of a medium of index of refraction  $n$ . It is at the average angle of incidence  $\theta$  from the unit normal  $\hat{n}$  to the interface, where  $\hat{n}$  points into the medium. In the figure the plane of the reflecting surface is considered vertical, and the horizontal projection of the packet's average wave vector is at an angle  $A$  from the normal  $\hat{n}$ . The fact that  $A$  and  $\theta$  can be different allows for the possibility that the path inside a prism can be helical. (For repeated reflections inside an equilateral triangular prism,  $A=30^\circ$ .) We choose a right-handed rectangular coordinate system  $(x, y, z)$  such that the  $z$  axis is parallel to the average direction of the incoming beam and the  $x$  axis is horizontal, at the angle  $\frac{1}{2}\pi - A$  from  $\hat{n}$ . Then for a particular Fourier component of the packet, one has a propagation vector,  $\vec{k} = (k_x, k_y, k_z)$ , with  $k_z \gg (k_x^2 + k_y^2)^{1/2}$ . It is assumed that the values of  $k_x$  and  $k_y$  are symmetrically distributed about zero in the packet. The magnitude of  $\vec{k}$  is  $k = n\omega/c$ .

In the  $(x', y', z')$  coordinate system, where  $y'$  is vertical and  $x'$  is in the reflecting plane (see Fig.

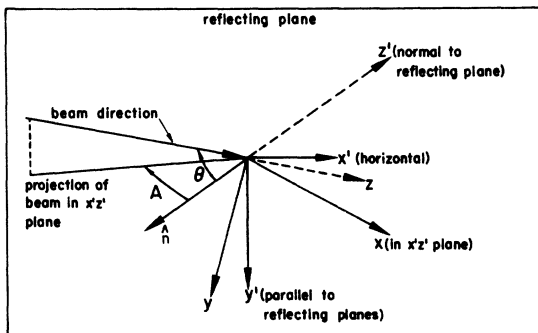


FIG. 1. Reflection geometry. The horizontal unit vector  $\hat{n}$  is normal to the vertical reflecting surface and points toward the region from which the beam is incident. The  $z$  axis is in the average beam direction and the  $x$  axis is horizontal. The  $x', y', z'$  coordinate axes are parallel or perpendicular to the reflecting surface, as indicated.

1), the components of  $\vec{k}$  are

$$\begin{aligned} k'_x &= (k_x \cos^2 A - \beta k_y \sin A + k_z \sin A \cos \theta) / \cos A, \\ k'_y &= (k_y \cos \theta + \beta k_x) / \cos A, \\ k'_z &= -k_x \sin A - \beta k_y + k_z \cos \theta, \end{aligned} \quad (1)$$

where  $\beta$  is given by

$$\beta = +(\cos^2 A - \cos^2 \theta)^{1/2}. \quad (2)$$

After reflection, the wave vector, denoted by  $\vec{k}''$ , is the same except for a reversal in sign of  $k'_z$ .

The effect of reflection is most easily discussed in terms of polarizations perpendicular and parallel to the plane of incidence. Unit polarization vectors normal to and in the plane of incidence are given, respectively, by

$$\begin{aligned} \hat{e}_N &= \frac{\vec{k} \times \hat{n}}{|\vec{k} \times \hat{n}|}, \\ \hat{e}_P &= \frac{\hat{e}_N \times \vec{k}}{k}. \end{aligned} \quad (3)$$

After one reflection, the electric field amplitudes  $E_N$  and  $E_P$  are multiplied by  $r_N$  and  $r_P$ , respectively, where

$$r_N = \frac{1 - R}{1 + R}, \quad (4)$$

$$r_P = \frac{1 - n^2 R}{1 + n^2 R}. \quad (5)$$

At incidence angles less than the critical angle,  $R$  is given by

$$R = \frac{1}{k'_z} (-k^2 + k'^2_z + k^2/n^2)^{1/2}, \quad (6)$$

while at incidence angles greater than the critical angle

$$R = \frac{i}{k'_z} (k^2 - k'^2_z - k^2/n^2)^{1/2}. \quad (7)$$

For angles of incidence greater than the critical angle for total internal reflection, the coefficients  $r_N$  and  $r_P$  may be put in the form of phase factors

$$r_N = e^{-2i\delta_N}, \quad r_P = e^{-2i\delta_P}, \quad (8)$$

where

$$\tan \delta_N = -iR, \quad \tan \delta_P = n^2 \tan \delta_N. \quad (9)$$

The polarization vectors of the reflected wave are

$$\begin{aligned} \hat{e}'_N &= \frac{\vec{k}'' \times \hat{n}}{|\vec{k}'' \times \hat{n}|} \\ &= \hat{e}_N, \\ \hat{e}'_P &= \frac{\hat{e}'_N \times \vec{k}''}{k}. \end{aligned} \quad (10)$$

After the first reflection let the reflected beam

be incident on a second vertical reflecting surface at the same average angle of incidence  $\theta$ , with respect to the second surface's unit normal vector  $\hat{n}''$ . The first and second surfaces intersect at the angle  $2A$ , and hence

$$(\hat{n}'' \times \hat{n})_{y'} = -\sin 2A. \quad (11)$$

Unit polarization vectors appropriate for the description of reflection at the second surface are given by

$$\begin{aligned} \hat{e}_N'' &= \frac{\vec{k}'' \times \hat{n}''}{|\vec{k}'' \times \hat{n}''|}, \\ \hat{e}_P'' &= \frac{\hat{e}_N'' \times \vec{k}''}{k}. \end{aligned} \quad (12)$$

In general, the polarization vectors  $\hat{e}_N''$  and  $\hat{e}_P''$  are rotated with respect to  $\hat{e}_N'$  and  $\hat{e}_P'$  by an angle  $B$ . Therefore a plane wave, which before reflection is a superposition of polarizations of the form

$$\vec{E} = E_N \hat{e}_N + E_P \hat{e}_P,$$

becomes, just before the second reflection,

$$\vec{E}'' = E_N'' \hat{e}_N'' + E_P'' \hat{e}_P''.$$

The amplitudes ( $E_N''$ ,  $E_P''$ ) are given by the  $2 \times 2$  reflection transformation matrix

$$\begin{aligned} \begin{pmatrix} E_N'' \\ E_P'' \end{pmatrix} &= \begin{pmatrix} r_N \cos B & -r_P \sin B \\ r_N \sin B & r_P \cos B \end{pmatrix} \begin{pmatrix} E_N \\ E_P \end{pmatrix} \\ &\equiv T \begin{pmatrix} E_N \\ E_P \end{pmatrix}. \end{aligned} \quad (13)$$

The effect of a series of reflections can then be represented by multiplying the amplitude ( $E_N''$ ,  $E_P''$ ) by a number of matrices of the form of  $T$ , one factor for each reflection. The coefficients  $r_N$  and  $r_P$  are given by Eqs. (4)–(7), and the angle  $B$  is given by

$$\begin{aligned} \sin B &= \hat{e}_P'' \cdot \hat{e}_N' \\ &= \frac{(\hat{k}'' \times \hat{n}'') \times \vec{k}''}{|\vec{k}'' \times \hat{n}''| k} \cdot \frac{\vec{k}'' \times \hat{n}}{|\vec{k}'' \times \hat{n}|} \\ &= \frac{-(\hat{n}'' \times \hat{n}) \cdot \vec{k}'' k}{|\vec{k}'' \times \hat{n}''| |\vec{k}'' \times \hat{n}|} \\ &= \frac{\sin 2A k'_x k}{D_+ D_-} \\ &= \frac{2k \sin A}{D_+ D_-} (k_y \cos \theta + \beta k_z), \end{aligned} \quad (14)$$

where

$$\begin{aligned} D_{\pm}^2 &= k_x^2 \cos^2 A + (1 - \beta^2) k_y^2 - k_z^2 \sin^2 \theta \\ &\quad + 2k_x k_z \beta \cos \theta \pm 2k_x \sin A (k_x \cos \theta - \beta k_y). \end{aligned} \quad (15)$$

To simplify the discussion, we shall assume that the source is a line parallel to the  $x$  axis, as in the experiments performed by Imbert.<sup>3,4</sup> Then one may assume  $k_x \equiv 0$  so that  $D_+ = D_-$ . In Sec. III the effects arising from nonzero  $k_x$  will be discussed. If the reflection is repeated  $m$  times with the same geometry for each reflection, succeeding reflections can be represented by the same reflection transformation matrix,  $T$ , and the state of the reflected wave is represented by a transformation matrix  $T^m$ .

The matrix  $T$  has eigenvalues  $\lambda$  given by

$$\begin{aligned} \lambda_{\pm} &= \frac{1}{2} \{ (\cos B)(r_N + r_P) \\ &\quad \pm i[4r_N r_P - (\cos^2 B)(r_N + r_P)^2]^{1/2} \}, \end{aligned} \quad (16)$$

with eigenfunctions proportional to

$$\begin{pmatrix} a_{\pm} \\ b_{\pm} \end{pmatrix} = \begin{pmatrix} r_P \sin B \\ r_N \cos B - \lambda_{\pm} \end{pmatrix}. \quad (17)$$

For incidence angles greater than the critical angle, the eigenvalues may be put in the form

$$\lambda_{\pm} = e^{\pm i\psi - i(\delta_P + \delta_N)}, \quad (18)$$

where

$$\cos \psi \equiv \cos B \cos(\delta_P - \delta_N). \quad (19)$$

The eigenvectors for  $\lambda_+$  and  $\lambda_-$  correspond in general to elliptically polarized light waves. Only when the angle of incidence is exactly equal to the critical angle for total internal reflection do the eigenfunctions correspond to left and right circularly polarized light beams, respectively. Wave packets constructed with only eigenvectors corresponding to  $\lambda_+$  give different transverse shifts than those constructed only with eigenvectors corresponding to  $\lambda_-$ . After  $m$  reflections, each eigenvector would be multiplied by the phase factor  $\lambda_{\pm}^m$ .

### III. CALCULATIONS OF THE TRANSVERSE SHIFT

If an expansion to first order in  $k_y$  of the phase of the eigenvalues given by Eq. (18) is a good approximation, then one may use the method of stationary phase to find approximate expressions for the final position of the image and hence of the transverse shift. For example, for metallic reflection we may set

$$\begin{aligned} \delta_P &= \delta_N \\ &= \frac{1}{2}\pi. \end{aligned}$$

Then  $\psi = B$  and thus to first order in  $k_y$ ,

$$\begin{aligned}\psi &\cong \sin^{-1} \left[ \frac{2k \sin A}{D_+ D_-} (k_y \cos \theta + \beta k) \right] \\ &\cong \sin^{-1} \left( \frac{2\beta \sin A}{\sin^2 \theta} \right) + \frac{2k_y \cos \theta \sin A}{k \sin^2 \theta}.\end{aligned}\quad (20)$$

Hence, after  $m$  reflections, right and left circularly polarized light beams are shifted in the positive and negative  $y$  directions, respectively, by

$$m \frac{2 \cos \theta \sin A}{k \sin^2 \theta}.\quad (21)$$

This is the same expression that was obtained by Schilling,<sup>8</sup> except that in Eq. (21) there is an additional factor,  $\sin A / \sin \theta$ , which arises from the assumed helical path.

In a prism of index of refraction  $n$ , if the angle of incidence is significantly greater than the critical angle, one can similarly expand the phase  $\pm\psi - (\delta_p + \delta_N)$  in Eq. (18) to first order in  $k_y$ . The terms arising from the expansion of  $\pm\psi$  then give rise to lateral splitting of the images, while the terms arising from  $-(\delta_p + \delta_N)$  give an over-all shift. The resulting expressions are lengthy, and will not be given here. However, in Fig. 2 these shifts are plotted for the eigenfunctions corresponding to  $\lambda_+$  for the particular case  $\lambda = 6328 \text{ \AA}$ ,  $n = 1.8$ ,  $m = 28$ ,  $A = 30^\circ$ . Near the critical angle for total internal reflection, indicated in the diagram by the vertical dashed line, the method of stationary phase breaks down and the shifts appear to approach infinity. However, the difference between the shifts, plotted as the dashed curve in Fig. 2, approaches a finite value at the critical angle;

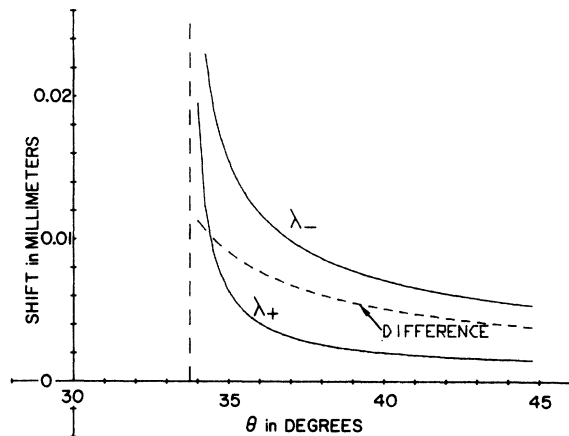


FIG. 2. Shifts in image position by the stationary phase method for the two eigenfunctions corresponding to  $\lambda_+$  and  $\lambda_-$ , for wavelength  $6328 \text{ \AA}$ ,  $n = 1.8$ ,  $m = 28$ ,  $A = 30^\circ$ . The vertical dashed line is at the critical angle for total internal reflection. The dashed curve is the difference between the two shifts.

this difference is given by

$$\Delta L_y = \Delta L_1 + \Delta L_2,\quad (22)$$

where

$$\Delta L_1 = m \frac{2\lambda \cos \theta \sin A}{\pi \sin^2 \theta},\quad (23)$$

and is essentially Schilling's result multiplied by  $\sin A / \sin \theta$  due to the assumed helical light path. The effect of the phases  $\delta_N$  and  $\delta_p$  gives an additional contribution to the splitting,

$$\Delta L_2 = m \frac{\lambda \cos^3 \theta (2 \sin^2 A - \sin^2 \theta)}{2\pi \sin^4 \theta \sin A}.\quad (24)$$

This result agrees with that of Boulware<sup>17</sup>; the total splitting  $\Delta L_y$  agrees closely with that of Imbert<sup>3</sup>

$$\Delta L_y = m \frac{\tan A}{\tan \theta} \frac{2\lambda}{\pi \sin \theta \cos \theta},\quad (25)$$

at the particular value of index of refraction ( $n = 1.8$ ) used in the experiment. In fact, at  $n = 1.78$  for  $A = 30^\circ$ , the expressions (22) and (25) are in exact agreement. However, at other values of  $n$  the two theories give different results; for example, at  $n = 1.5$  with  $\theta$  and  $A$  nearly equal, Imbert's expression, Eq. (25), predicts a splitting about 40% greater than is predicted by the Eqs. (22)–(24) obtained here and by Boulware.<sup>17</sup>

Also, Imbert's formula gives equal and opposite shifts for the two polarizations, whereas it may be seen from Fig. 2 that both shifts are positive. The reason both images are shifted in the positive  $y$  direction is that, in the exponent  $-i(\delta_p + \delta_N)$  of Eq. (18), when  $A \neq \theta$  there arise terms proportional to  $k_y$  for small  $k_y$ .

Because the stationary phase method breaks down near the critical angle, it was felt that more extensive numerical calculations were necessary in order to predict the lateral shift of the image of a line source; therefore, computer calculations were performed to find the intensity distribution in the image. The incident-wave packet was assumed to consist of a superposition of plane waves with the amplitudes weighted by the exponential function

$$f(k_y) = \frac{1}{2} \sigma e^{-\sigma |k_y|}.\quad (26)$$

The incident wave is thus written

$$\int_{-\infty}^{\infty} dk_y f(k_y) \exp[i(k_y y + k_z z - \omega t)] [\hat{e}_N(\vec{k}) \pm i \hat{e}_P(\vec{k})] \sqrt{2},\quad (27)$$

where the  $\pm$  signs correspond to right and left circularly polarized light beams, respectively. In terms of the eigenfunctions, Eq. (17), the polar-

ization vectors can be written in matrix form:

$$\frac{1}{\sqrt{2}} \begin{pmatrix} 1 \\ \pm i \end{pmatrix} = C_+ \begin{pmatrix} a_+ \\ b_+ \end{pmatrix} + C_- \begin{pmatrix} a_- \\ b_- \end{pmatrix}, \quad (28)$$

where

$$C_+ = \frac{b_- \mp ia_-}{\sqrt{2}(a_+b_- - a_-b_+)}, \quad (29)$$

$$C_- = \frac{-(b_+ \mp ia_+)}{\sqrt{2}(a_+b_- - a_-b_+)}. \quad (30)$$

After  $m$  reflections, the wave packet is modified in such a way that

$$\begin{aligned} C_+ &\rightarrow \lambda_+^m C_+, \\ C_- &\rightarrow \lambda_-^m C_-, \end{aligned} \quad (31)$$

so the final wave packet is

$$\begin{aligned} &\int dk_y f(k_y) \exp[i(k_y y + k_x z - \omega t)] \\ &\times [\lambda_+^m C_+ (a_+ \hat{e}_N + b_+ \hat{e}_P) + \lambda_-^m C_- (a_- \hat{e}_N + b_- \hat{e}_P)]. \end{aligned} \quad (32)$$

This integration was performed separately at  $z = 0$  for right and left circularly polarized light beams corresponding to the  $\pm$  signs in Eq. (27), for  $\lambda = 6328 \text{ \AA}$ ,  $n = 1.8$ ,  $m = 28$ ,  $A = 30^\circ$ ,  $\sigma = 30/k$ , and average incidence angle at the critical angle. The results are plotted in Fig. 3 on a horizontal scale expanded by a factor of 300, corresponding to the magnification used by Imbert.<sup>3</sup> These distributions are much like the images obtained by Imbert. The distance between peaks is comparable to the splitting in Fig. 2 at the critical angle. However, be-

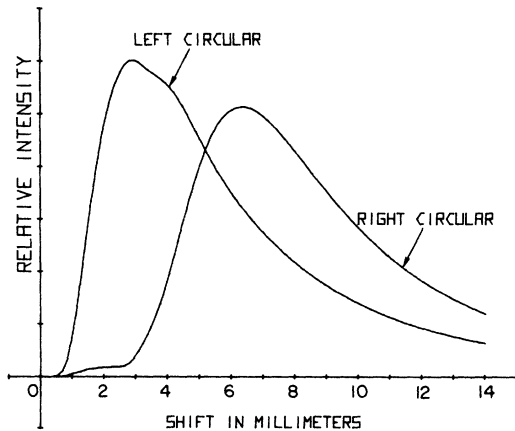


FIG. 3. Numerically calculated intensities for left and right circularly polarized light beams of wavelength  $6328 \text{ \AA}$ , for  $m = 28$  reflections,  $n = 1.8$ ,  $A = 30^\circ$ , and exponential weighting function characterized by  $\sigma = 30/k$ ; the average angle of incidence is the critical angle. The horizontal scale has been magnified by a factor of 300.

cause of the great widths of the images, it is difficult to compare the splitting with experimental results without knowing the details of the experimental analysis of the photographic images. The widths of these curves are not due to our choice of  $\sigma$ , but rather are due to the fact that near the critical angle, the exponent  $-i(\delta_P + \delta_N)$  in Eq. (18) is proportional to  $\sqrt{k_y}$  for small  $k_y$ . This causes broadening of the images and is also the source of the breakdown of the stationary-phase method.

An alternative experimental arrangement has been reported by Imbert<sup>4</sup> with incident unpolarized light, in which after 28 reflections the beam was analyzed into right and left circularly polarized components. Numerical calculations using wave packets similar to those in Eq. (32) have been performed in which the outgoing eigenfunctions are analyzed into right and left circular polarizations, with averaging over initial phases. The results differ from those shown in Fig. 3 by only a few parts in  $10^4$ . This slight difference arises from the fact that the eigenfunctions do not in general correspond to circularly polarized light.

It is also of interest to investigate the case in which the average plane of incidence is horizontal, so that  $\theta = A$ , since then  $\delta_P$  and  $\delta_N$  are proportional to  $|k_y|$  rather than  $\sqrt{k_y}$  for small  $k_y$ . The resulting intensity distribution after optical multiplication by a factor of 300 is plotted in Fig. 4 for the case of 28 reflections, wavelength in vacuum  $6328 \text{ \AA}$ , and index of refraction  $n = 1.8$  as in Imbert's experiment.<sup>3</sup> The solid curve corresponds to reflection with the centroid of the incident beam at the critical angle,  $\sin\theta = 1/n$ , and with the beam spread determined by  $\sigma = 10/k$ . In this case, with  $k_x = 0$  the tangents of the phase shifts are linear in  $|k_y|$ :

$$\begin{aligned} \tan\delta_N &= |k_y|/k, \\ \tan\delta_P &= n^2 |k_y|/k. \end{aligned} \quad (33)$$

On the other hand, the dotted curve in Fig. 4 corresponds to  $\sigma = 30/k$ , with the centroid of the incident beam incident at an angle  $10'$  greater than the critical angle. The shift is greatly decreased in this case. Similarly the shift would also be greatly decreased if the beam were localized in the  $x$  direction, requiring a distribution of values of  $k_x$  in the wave packet. The reason is that  $k_x$  occurs linearly and  $k_y$  occurs quadratically in the square root appearing in Eq. (7), for  $R$ . Then for small  $k_y$ , the linear term in  $k_x$  is the more important term. On the other hand, if  $A \neq \theta$ , as long as the spread of values of  $k_x$  occurring in the packet is somewhat less than the spread of  $k_y$ , the transverse shift will not be affected appreciably. This is because in Eq. (7) for  $R$ , when  $k_x$

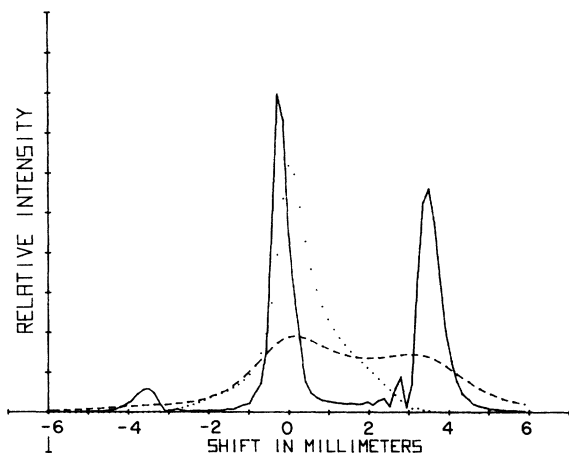


FIG. 4. Numerically calculated intensities for right circularly polarized light beams of wavelength  $6328 \text{ \AA}$  for  $m=28$  reflections,  $n=1.8$ , and  $A=\theta$ . An exponential weighting function has been used. The solid curve corresponds to  $\sigma=10/k$ , reflection at the critical angle; the dotted curve corresponds to  $\sigma=30/k$ , and an angle of incidence  $10'$  greater than the critical angle. The dashed curve corresponds to  $\sigma=90/k$  with reflection at the critical angle.

and  $k_y$  are small, both  $k_x$  and  $k_y$  occur linearly under the square root. Owing to the fact that the sign of  $k_x$  effectively changes at each reflection, after two reflections the linear terms in  $k_x$  in the eigenvalues  $\lambda_{\pm}$  cancel; the eigenvalues then depend quadratically on  $k_x$  and linearly on  $k_y$ , and the linear terms in  $k_y$  are the more important.

The dashed curve in Fig. 4 corresponds to reflection at the critical angle with  $\sigma=90/k$ . Left circularly polarized light would give images identical to those in Fig. 4, but reflected about the vertical axis; thus unpolarized light would give rise to a number of peaks. If Gaussian weighting factors were used instead of exponentials in construction of the wave packets, Figs. 3 and 4 would be substantially the same. From these curves it is clear that there is no single simple formula for the transverse shift near the critical angle.

It has been suggested that simultaneous observation of the longitudinal and transverse shift is impossible because they would have to be focussed in different ways.<sup>14</sup> Actually it should be pointed out that with multiple reflections there can be no longitudinal shift for the geometry discussed above

because, as noted previously, the eigenvalues  $\lambda_{\pm}$  (after two reflections) are even functions of  $k_x$ . There is no linear  $k_x$  term in the exponent of  $\lambda_{\pm}$ , so there can be no net shift in the  $x$  direction for any even number of reflections.

Furthermore, when the geometry of the reflecting planes is such that the longitudinal shift is observable, there can be no transverse shift. Thus consider the process of multiple reflection between parallel planes of a plane wave with wave vector  $(k_x, k_y, k_z)$ . In this case we may take  $A=\theta$ ,  $\beta=0$ , and the normals  $\hat{n}$  and  $\hat{n}''$  point in exactly opposite directions. Clearly then the angle  $B$  vanishes, and the  $2 \times 2$  reflection transformation matrix becomes diagonal. The eigenfunctions of the reflection process are then linearly polarized parallel and perpendicular to the plane of incidence. With the choices of axes shown in Fig. 1, the wave vector of the wave incident on the second reflecting surface is  $(k_x, -k_y, k_z)$ . After two reflections the wave vector incident on the third surface will be  $(k_x, k_y, k_z)$  and the wave amplitude will be multiplied by  $e^{-4i\delta_N}$  or  $e^{-4i\delta_P}$ , as the angles  $\delta_N$  and  $\delta_P$  are even functions of  $k_y$ . Since there are no terms linear in  $k_y$  in the phases  $\delta_N$  and  $\delta_P$ , there will be no transverse shift. Thus we conclude that the longitudinal and transverse shifts cannot be observed simultaneously.

#### IV. CONCLUSIONS

While the results obtained in this paper for the splitting between the transversely shifted images generally are in agreement with experiment, several new aspects of the phenomenon have been demonstrated. First, it has been shown that both images can be shifted in the same direction in disagreement with the predictions of Costa de Beauregard, Imbert, Ricard, and Schilling. Second, the agreement between the present calculations and those of Imbert for the splitting between the images is coincidental; this agreement occurs only for an index of refraction  $n \cong 1.8$ , which was used in the experiment. These results suggest that more experiments should be performed with different indices of refraction, and that some effort should be made to detect the asymmetry in the shifts, possibly by comparing images at different wavelengths.

- <sup>1</sup>F. Goos and M. Hänchen, *Ann. Phys. (Paris)* 1, 333 (1947).
- <sup>2</sup>F. I. Fedorov, *Dokl. Akad. Nauk. SSSR* 105, 465 (1955).
- <sup>3</sup>C. Imbert, *Phys. Rev. D* 5, 787 (1972).
- <sup>4</sup>C. Imbert, *Compt. Rend.* B274, 1213 (1972).
- <sup>5</sup>K. Artmann, *Ann. Physik* 2, 87 (1948).
- <sup>6</sup>J. L. Agudin, *Phys. Rev.* 171, 1385 (1968).
- <sup>7</sup>H. K. V. Lotsch, *Optik* 32, 116 (1970); 32, 189 (1970); 32, 299 (1970); 32, 553 (1970). The last article in this series contains an extensive list of references on the Goos-Hänchen effect.
- <sup>8</sup>H. Schilling, *Ann. Physik* 16, 122 (1965).
- <sup>9</sup>O. Costa de Beauregard, *Phys. Rev.* 139, B1446 (1965).
- <sup>10</sup>J. Ricard, *Nouv. Revue d'Optique* 1, 275 (1970).
- <sup>11</sup>C. Imbert, *Compt. Rend.* B267, 1401 (1968).
- <sup>12</sup>L. de Broglie and Jean-Pierre Vigier, *Phys. Rev. Letters* 28, 1001 (1972).
- <sup>13</sup>G. J. Troup, J. L. A. Francey, R. G. Turner, and A. Tirkel, *Phys. Rev. Letters* 28, 1540 (1972).
- <sup>14</sup>O. Costa de Beauregard, *Lett. Nuovo Cimento* 3, 613 (1972); O. Costa de Beauregard and C. Imbert, *Phys. Rev. Letters* 28, 1211 (1972).
- <sup>15</sup>J. D. Jackson, *Classical Electrodynamics* (Wiley, New York, 1962), pp. 216 ff.
- <sup>16</sup>S. C. Miller and N. Ashby, *Phys. Rev. Letters* 29, 740 (1972).
- <sup>17</sup>D. G. Boulware, this issue, *Phys. Rev. D* 7, 2375 (1973).